Numerical Navier-Stokes Solutions of High-Speed Propeller Flows

S. J. Yoon* and J. A. Schetz†
Virginia Polytechnic Institute and State University, Blacksburg, Virginia

Abstract

THE search for improved fuel economy for subsonic aircraft has led to a renewed interest in propeller aerodynamics. There is a need for detailed aerodynamic analysis of the flow near and behind the propeller, including the effects of an engine nacelle to refine propeller and nacelle design and assess slipstream effects on the other components of the aircraft. The available data for flowfield details are quite limited.

The flow near and behind the propeller is turbulent, and the downstream variation of the swirl, etc., is dominated by viscous effects. Previous detailed analysis for high-speed cases have been limited by an inviscid flow assumption.

The goal of this work has been to extend detailed viscous analysis of propeller flows into the high-speed regime. The complete three-dimensional, periodic, unsteady, turbulent problem involved in the real case is too complex and large to be attacked at this time. Some simplifying assumptions were necessary. First, the flow was taken as axisymmetric. Second, and very important, the propeller has been represented by an actuator disk. The disk can be located arbitarily in space, so that the effects of propeller sweep can be included. Also, arbitrary radial variations of the thrust and torque are permitted.

The calculations were made with a finite-difference solution of the compressible, axisymmetric (with swirl), Reynolds-averaged, turbulent Navier-Stokes equations.

Contents

Simulation of the Propeller

The effect of the propeller, as modeled here, appears through an axial force term $F_x(r)$ and a peripheral torque term $F_\theta(r)$. The only information that is usually available consists of propeller performance curves for uniform inflow and the rpm of the propeller in its operating condition with a body or nacelle. A simple blade-element propeller analysis can be used to estimate the appropriate radial distributions.

Turbulence Modeling

For the present case, an anisotropic model was not employed because preliminary calculations showed that the swirl level produced by a turboprop is quite weak.

The mixing length model chosen here is the Launcher et al model for free shear layers, with velocity maxima or minima

$$\ell_m = C_{ML} \cdot b$$

where $b$is the width of the mixing zone and the proportionality constant C_{ML} is 0.11 for axisymmetric flows. Launder selects the mixing length on the basis of the axial velocity profiles. For propeller flows, and especially for cases with an engine nacelle, it was found to be advantageous to work with the swirl velocity profiles.

Presented as AIAA 86-1538 at the AIAA/ASME/SAE/ASEE 22nd Joint Propulsion Conference, Huntsville, AL, June 16-18, 1986; received July 22, 1986; synoptic received Oct. 5, 1987. Full paper available at AIAA Library, 555 W. 57th St., New York, NY 10019. Price: microfiche, $4.00; hard copy, $9.00. **Remittance must accompany order.**

*Graduate Assistant, Aerospace and Ocean Engineering Dept. Student Member AIAA.

†W. Martin Johnson Professor and Dept. Head, Aerospace and Ocean Engineering Dept. Fellow AIAA.

Boundary Conditions

The inflow was taken as uniform. All of the unspecified dependent variables are computed from characteristic relations. The viscous terms are treated as source terms.

For the lateral bounding cylindrical surface, the static pressure was specified. If the flow across the boundary is outflow, the remaining variables are determined by the characteristic relations. If inflow occurs, the velocity components tangent to the boundary and the density are specified. The normal velocity component is determined using the characteristic relations.

The outflow boundary conditions were determined by linear extrapolation of all of the dependent variables.

We do not try to resolve the wall boundary layer on the nacelle with the full Navier-Stokes formulation. The wall boundary condition used was the free slip condition.

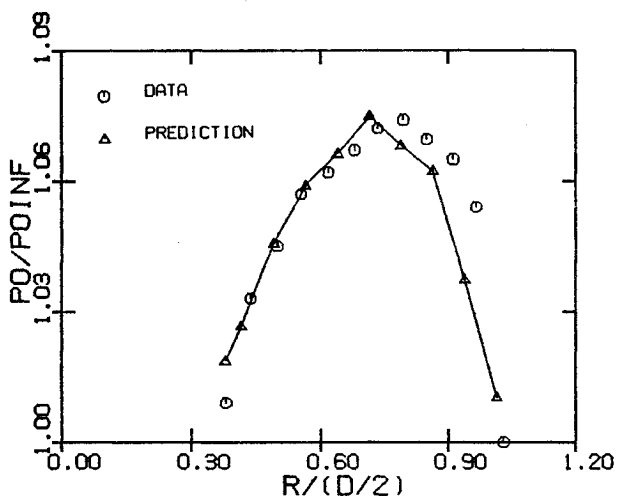

Fig. 1 Comparison of stagnation pressure profiles at $X/D \sim 0.1$ for SR1.

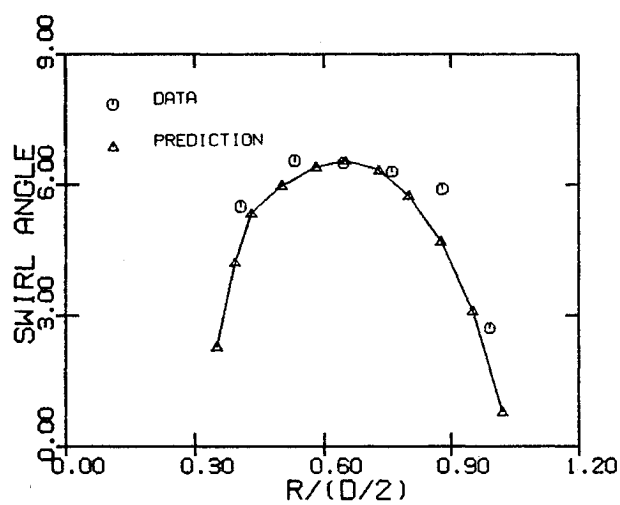

Fig. 2 Comparison of swirl velocity profiles $X/D \sim 0.1$ for SR1.

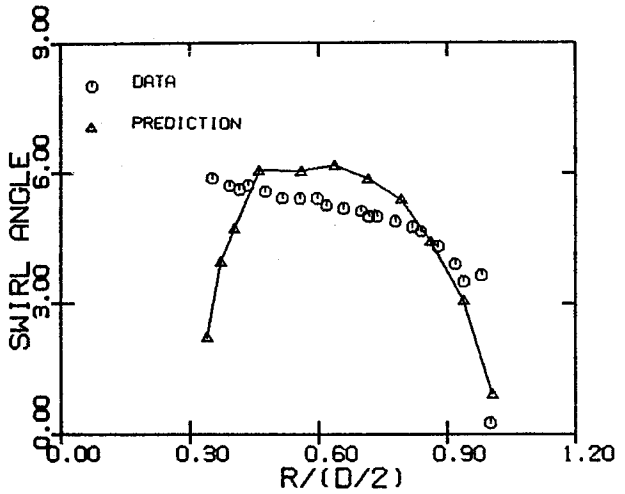

Fig. 3 Comparison of swirl velocity profiles at $X/D \sim 0.1$ for SR3.

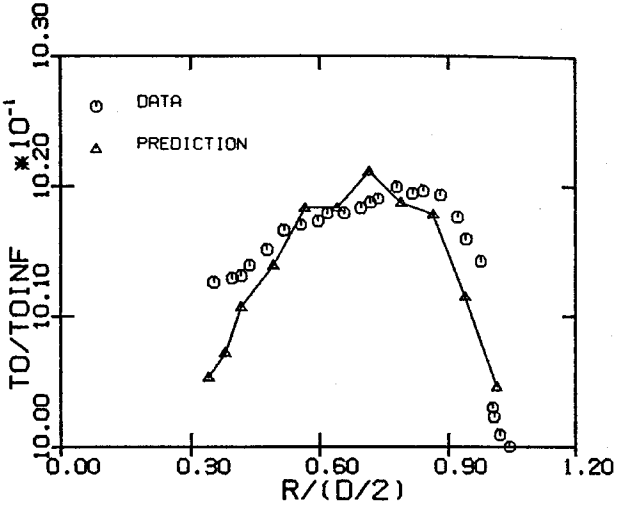

Fig. 4 Comparison of stagnation temperature profiles at $X/D \sim 0.1$ for SR3.

Numerical Methods

The numerical method used for this work is the explicit, unsplit MacCormack scheme. This finite-difference scheme is two-step, uncentered, and second-order accurate. Backward differences are used for the predictor step, and forward differences are used for the corrector step. This scheme was chosen because it is accurate and well tested.

A 41 × 25 nonuniform grid was used. This grid size and spacing were selected after numerous trial calculations for similar problems.

Results and Discussion

To test the adequacy of the predictions, we have selected NASA/Hamilton standard SR1 and SR3 propellers as test cases for comparison.

For the SR1 propeller, the operating conditions for the case selected are

$$J = 3.12,\ C_P = 1.73,\ C_T = 0.429,\ M_\infty = 0.8$$

No axial velocity test data are available for comparison with the numerical predictions. The only related data given is a radial stagnation pressure profile at $x/D \sim 0.1$. A comparison of predictions and measurements is plotted in Fig. 1. The agreement is generally quite good. The largest discrepancy is in the region toward the blade tips. The profile for the stagnation pressure shows some nonsmoothness. This is primarily a result of the fact that this quantity is postcalculated from the computational dependent variables of static pressure, density, and velocity. A comparison of predictions and measurements for the swirl component at the same station is shown in Fig. 2. Generally good agreement is indicated here also.

For the SR3 test case selected,

$$J = 3.002,\ C_P = 1.385,\ C_T = 0.38,\ M_\infty = 0.8$$

The experimental data available are only stagnation temperature and swirl velocity profiles at $x/D \sim 0.1$. The swirl prediction is poor near the root but reasonably good elsewhere. The stagnation temperature profile agrees well with the data in the midzone but less well near the root and tip. The nonsmoothness of the stagnation temperature profile is again caused by postcalculation to determine this quantity from the computed pressure, density, and velocity.